

# Mechanisms of Laser-Tissue Interaction:

## II. Tissue Thermal Properties

Mohammad Ali Ansari, Mohsen Erfanzadeh, Ezeddin Mohajerani

Laser and Plasma Research Institute, Shahid Beheshti University, Tehran, Iran

### Abstract:

Laser-tissue interaction is of great interest due to its significant application in biomedical optics in both diagnostic and treatment purposes. Major aspects of the laser-tissue interaction which has to be considered in biomedical studies are the thermal properties of the tissue and the thermal changes caused by the interaction of light and tissue. In this review paper the effects of light on the tissue at different temperatures are discussed. Then, due to the noticeable importance of studying the heat transfer quantitatively, the equations governing this phenomenon are presented. Finally a method of medical diagnosis called thermography and some of its applications are explained.

**Keyword:** Lasers; Tissues; Absorptions

---

Please cite this article as follows:

Ansari MA, Erfanzadeh M, Mohajerani E. Mechanisms of Laser-Tissue Interaction: II. Tissue Thermal Properties. *J Lasers Med Sci* 2013; 4(3):99-106

---

\***Corresponding Author:** Mohammad Ali Ansari, PhD; Laser and Plasma Research Institute, Shahid Beheshti University, Tehran, Iran; Tel: +98-2129904014; Fax: +98-2122431775; Email: m\_ansari@sbu.ac.ir

### Introduction

As it was emphasized in the previous review article<sup>1</sup>, lasers are widely used in biology and medicine and the majority of the hospitals utilize modern laser systems for diagnostic and therapeutic applications. The medical laser applications are defined by the type of interaction between laser light and tissues. Knowledge of laser-tissue interaction can help doctors or surgeons to select the optimal laser systems and to modify the type of their therapy<sup>1-3</sup>. Therefore, we seek to review the mechanisms of laser-tissue interaction. In reference number 1, the optical properties of biological tissue such as absorption, scattering, penetration and fluorescence have been reviewed<sup>1</sup>. In this paper, we intend to study the thermal properties of the biological tissues. During all medical applications based on heating such as hair removal, cancer therapy or laser-induced interstitial thermotherapy (LITT), it is desirable to have a complete knowledge of temperature distribution in the tissue. Study of this temperature distribution requires knowledge about the thermal properties of biological

tissues. The transportation of thermal energy in biological tissues is a complicated procedure including different phenomenological mechanisms such as thermal conduction, convection, radiation, metabolic activities and phase change<sup>2</sup>. If a biological tissue is illuminated by a laser light such as Neodymium-Doped Yttrium Aluminium Garnet (Nd:YAG) or Carbon Dioxide (CO<sub>2</sub>) laser, one can see multiple effects like coagulation, vaporization, carbonization or melting. These effects depend on the peak power and wavelength of the laser as well as the thermal properties of biological tissues. In Figures 1-5, these thermal effects are shown.

In 1967 Dr. Kelly published the first paper about laser coagulation. He applied laser for pre-retinal haemorrhage on rabbits and he emphasized that for higher energy setting, the nerve-fibre of retina maybe destroyed<sup>3</sup>. Laser can increase the temperature of cells and it results in denaturation of proteins and collagen that leads to coagulation of tissue and it can necrotize cells. The red blood cells tend to absorb green light, hence green light laser is a good choice for diabetic eyes (Figure 1).



**Figure 1.** Coagulation of a diabetic retina by a potassium-titanyl-phosphate Neodymium-Doped Yttrium Aluminium Garnet (KDP-Nd:YAG) laser beam.

### Heat effects

Increasing the body temperature leads to several effects such as hyperthermia, coagulation and

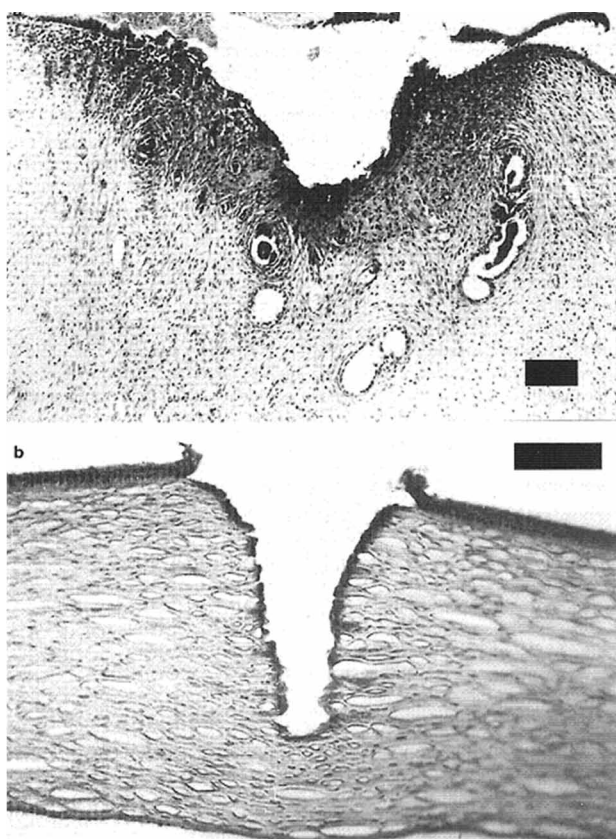


**Figure 2.** (a) Uterine tissue of a wistar rat coagulated with CW Nd:YAG laser(power: 10 W, bar: 80 micron) and (b) Human cornea coagulated with 120 pulses from an Erbium-Doped Yttrium Aluminium Garnet (Er:YAG) laser(pulse duration: 90 microsecond, pulse energy: 5 mJ, 1Hz, bar: 100 micron)<sup>2</sup>.

other irreversible tissue effects. By increasing the temperature, the initial effect is hyperthermia. The typical range of 40-50 degrees Celsius is called hyperthermia domain within which some molecular bonds are destroyed and the membrane is altered. The reduction in enzyme activity is observed. However, the effects in this temperature range are reversible.

For temperatures around 60°C, denaturation of proteins and collagen occurs which leads to the coagulation of tissue and it can necrotize cells. Several optical treatments such as LITT and hair removal aim at temperatures above 60°C. At higher temperature the equilibrium of chemical concentration is destroyed as the permeability of membrane of cells increases.

The vaporization of water occurs at 100°C. The vaporization is sometimes referred to as the thermomechanic procedure, because within the vaporization phase, the temperature of tissue does not alter and gas bubbles are formed. The propagation of these bubbles accompanied with the alteration of their volume causes thermal decomposition of tissue

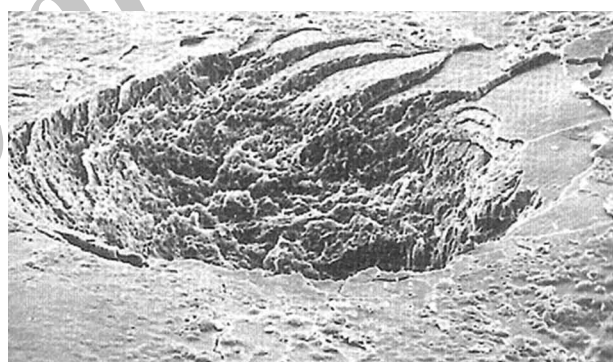


**Figure 3.** Human tooth vaporized with 20 pulses from an Er:YAG laser (pulse duration: 90 microsecond, pulse energy: 100 mJ, 1 Hz)<sup>2</sup>

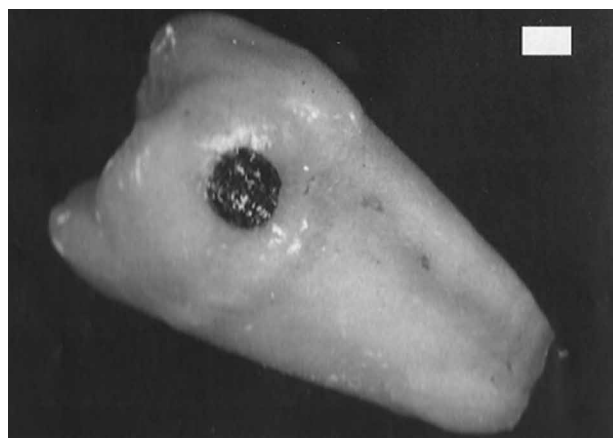


**Figure 4.** Human tooth carbonized with Continues-wave (CW) CO<sub>2</sub> laser (power 1 W, bar: 1 mm)<sup>2</sup>.



**Figure 5.** Human tooth melted with 100 pulses from a Ho: YAG laser (pulse duration: 3.8 microsecond, pulse energy: 18 mJ, 1 Hz)<sup>2</sup>.

**Table 1.** Thermal effects of laser light for different temperatures<sup>2</sup>.

Temperature	Biological effects
37°C	Normal
45-50°C	Hyperthermia, Reduction of enzyme activity, Cell immobility
60-80°C	Denaturation of proteins and collagen; Coagulation
100°C	Vaporization, Thermal decomposition(ablation)
>100°C	Carbonization
>300°	Melting

fragments. If all water molecules are vaporized, carbon atoms are released and the adjacent tissues are blackened and smoke rises from the skin. This stage is called carbonization (Figure 4). Finally beyond 300°C melting might occur (Figure 5). Table 1 depicts the summarized heat effects for different temperatures.

It is worth mentioning that 60°C is a critical temperature since most biological effects which occur at temperatures higher than that are irreversible.

## Heat transport

The energy of laser can be absorbed by targets such as water, melanin and blood. This absorbed energy leads to a raise in the temperature of tissue. This energy can be assumed as heat energy source. The heat source,  $S(r, z, t)$ , inside the exposed tissue is a function of absorption coefficient  $a$  and the laser intensity  $I(r, z, t)$ . In this regards heat conduction and heat convection are important as they transfer the heat energy inside tissue. The physics of heat transfer is complicated; therefore we only explain some important results. One of the important parameters is relaxation

time. Relaxation time is a time during which heat energy can diffuse inside tissue. The relaxation time is a function of extinction coefficient. Before we define relaxation time, the thermal penetration depth, which is another critical parameter that must be considered, shall be defined as:

$$z_{therm}(t) = \sqrt{4\kappa t} \quad (1)$$

In this equation  $\kappa$  is called temperature conductivity and its value is approximately the same for water  $1.4 \times 10^{-7} m^2/s$  according to reference number 2. Table 2 shows the thermal penetration depth, which is defined as a distance in which the temperature decreases to 63% of its peak value. This table expresses the thermal-temporal response of water; one shall keep in mind that heat diffuses in water up to approximately 0.7 micron within 1.0 microsecond. As it was expressed in reference number 1, the penetration depth, defined as  $L = 1/a$ , is a distance in which the intensity of laser has decreased to 63% of its peak value<sup>1</sup>. Experiments show that the relaxation time ( $\tau_{relax}$ ) of water at the absorption peak which is for a wavelength near 3 microns is 1.0 microsecond. If the laser pulse duration  $\tau$  is smaller than the relaxation time ( $\tau < \tau_{relax}$ ), the thermal energy cannot diffuse to the penetration depth; therefore thermal effects can be negligible. Heat can be diffused up to the optical penetration depth when  $\tau > \tau_{relax}$ , hence thermal effects or damages are possible. The criterion  $\tau_{relax} = 1 \mu s$  is useful for wavelength of 3.0 micron, however for visible laser light  $\tau_{relax}$  is larger than 270 hours! This is not extraordinary, because water is transparent for visible laser light. Relaxation time for near infra red (NIR) laser is smaller than 1.0 millisecond. One can calculate the relaxation time of different tissue by the following relation:

$$\tau_{relax} = \frac{1}{5.6 \times 10^{-7} a} \quad (2)$$

Because most medical applications of heat are transient, the tissue thermal diffusivity is important. In the following sections, we will introduce the important thermal parameters of biological tissues. As mentioned

**Table 2.** Thermal penetration depths of water <sup>2</sup>.

Time $t$	Thermal temperature depth $Z_{therm}(t)$
1 $\mu s$	0.7 $\mu m$
10 $\mu s$	2.2 $\mu m$
100 $\mu s$	7.0 $\mu m$
1 $ms$	22.0 $\mu m$
10 $ms$	70.0 $\mu m$



**Table 3.** Blood perfusion rates of some human organs<sup>2</sup>.

Tissue	Perfusion rate (ml /min g)
Fat	0.012-0.015
Muscle	0.02-0.07
Skin	0.15-0.2
Brain	0.46-1.0
Thyroid gland	~ 4.0

before, heat conduction and heat convection are important means of heat transfer. One typical example of heat conduction in tissue is the heat transfer by neighbourhood cells. The blood perfusion is an agent for heat convection; table 3 shows the perfusion rate of some human organs. It is worth stating that this perfusion rate is negligible in the first approximation, but for long exposure or LITT it has a significant role.

Heat conduction can be stated as following:

$$J = -k\nabla T \quad (3)$$

In this equation  $k$  is called heat conductivity and is expressed in units of  $W/mK$ .  $J$  is called heat flow. The value of heat conductivity at  $37^\circ C$  is  $0.63 W/mK$ . According to the equation of continuity the time evaluation of heat content per unit volume ( $\frac{\partial q}{\partial t}$ )

is determined by the divergence of the heat flow  $J$ :

$$\nabla J = -\frac{\partial q}{\partial t} \quad (4)$$

After some mathematics it is derived that:

$$\nabla^2 T(r, z, t) = -\frac{\rho c}{k} \frac{\partial T}{\partial t} + S(r, z, t) \quad (5)$$

Equation 5 is heat transfer equation. The transfer of heat in biological tissues can be modelled by this differential equation. The source term  $S(r, z, t)$  contains the term of perfusion, conduction and laser source. It has been shown in the literature that the duration pulse of 1.0 microsecond is a crucial parameter and the thermal effects and hence heat transfer equation must be studied by this parameter.

For temperatures above  $60^\circ C$ , the necrosis can happen. To obtain the number of the remaining active cells at a certain temperature level ( $C(t)$ ), we can use Arrhenius

$$\text{equation: } -\ln \frac{C(t)}{C_0} = A \int_0^t \exp\left(-\frac{e}{RT(t')}\right) dt' \equiv \Pi \quad (5)$$

$C_0$  is the initial concentration of cells,  $A$  is the Arrhenius constant,  $e$  and  $\Pi$  are specific tissue parameters and  $R$  is the universal gas constant. The local damage of tissue can be determined by this relation:

$$\begin{aligned} -h \frac{C(t)}{C_0} &= \Pi \\ \frac{C_0 - C(\text{Damage})}{C_0} &= -\exp(\Pi) \\ \frac{C(\text{Damage})}{C_0} &= 1 - \exp(\Pi) \end{aligned} \quad (6)$$

## Thermography

Nowadays, the researchers look for new non-invasive biomedical imaging methods. Among biomedical imaging, thermography is a non-invasive, non-contact skin surface temperature screening technique which is cost-effective, fast and does not cause any pain on the patient<sup>8</sup>. It is a relatively simple imaging approach that detects the variation of temperature on the human surface.

Ammer in 1995 showed that the thermography can be used to image muscle; Low activity muscles caused by neurological deficit or by pain inhibition should result in an asymmetric thermal pattern with low temperature over non-functioning muscles. Thermograms of 50 patients with pain in one ankle joint were re-evaluated for thermal asymmetry over the lower leg. Thirty-eight patients showed a pathological side-to-side difference of temperature over the ankle joint in a range of -1.8 to 3.4 degrees. Thermal asymmetry of the anterior lower leg, defined as side-to-side difference greater than 0.5 degrees was observed in 54% of patients. Nearly all of those patients showed a decrease of temperature (mean of temperature on the affected minus temperature of the healthy side:  $-0.32 \pm 0.78$ ) on the symptomatic side. A similar decrease of temperature over the muscles of the anterior lower leg was found in a small group of 10 patients with palsy of the peroneal nerve. Muscular inactivity should be considered as a reason for regions of low temperature in patients with painful ankle joints<sup>4</sup>.

Thermography is utilized in various medical fields reported in reference numbers 5-40 such as the detection of breast cancer, which is the refocus of many biomedical researchers in recent years<sup>5-40</sup> (Figure 6). The earliest breast thermogram was reported by Lawson<sup>41-44</sup>. He observed that the venous blood draining the cancer site is often warmer than its arterial supply. However, these measurements have never been confirmed by other groups and the findings might thus have been questionable. Thermograms

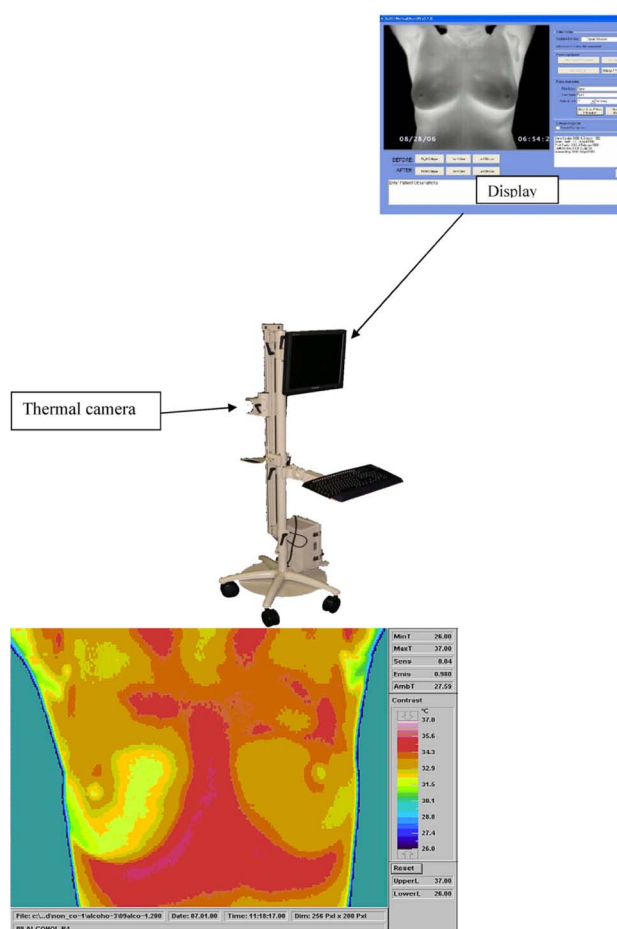


**Figure 6.** A thermal imaging setup for breast imaging (left picture) and Typical thermogram of an asymptomatic volunteer age 35 (right picture)<sup>4</sup>

alone will not be adequate for the medical practitioner to make a diagnosis. Analytical tools such as bio-statistical methods and artificial neural network are recommended to be included to study the thermogram objectively<sup>34,45-65</sup>. Notice that these approaches may improve the interpretation of thermal images which may lead to a higher diagnostic accuracy of infrared thermography, but these methods of analysis are not more objective than other highly accurate and precise measurement methods. With the rising use of thermal imaging, there is a need to have regulations and standards to provide accurate and consistent results. The standards are mainly based on the physics of radiation and thermoregulation of the body<sup>4</sup>.

Figure 6 illustrates a typical thermal imaging with an asymptomatic volunteer (aged 35) thermogram. Based on mammographic examinations in 1000 Singapore women on the eve of the breast cancer awareness month -Oct. 1998<sup>12,66</sup>, the average size of a cancerous lump<sup>58</sup>

was 1.415 cm in spheroid shape when detected in the clinic for the first time<sup>4</sup>. Temperature data are extracted from the breast thermograms. The thermograms consist of many colored pixels, each representing a temperature. From the thermograms, it is possible for an experienced medical practitioner to diagnose abnormalities such as a cyst. After every pixel's temperature is compiled, bio-statistical technique can be used to treat them, such as determining the mean, median and modal temperature of the breast region<sup>56</sup>.

Aweda showed that the Thermographic technique and energy exchange processes in 107 cancer patients were studied in order to determine relevance in cancer management<sup>5</sup>. The mean oxygen consumption rate in control subjects (36.13 ml/s) was higher than the mean oxygen consumption rate in breast (31.89 ml/s), head and neck (30.64 ml/s), cervical (28.05 ml/s) and other forms of cancers (30.78 ml/s). Mean metabolic heat production rate in control subjects (150.71 J/h) was higher than the mean metabolic heat production in breast (133.04 J/h), head and neck (127.80 J/h), cervical (117.00 J/h) and other cancers (128.37 J/h). Convective rate of heat exchange was -14462.91 J/h for non-cancer persons while it was -15841.98 J/h for breast, -15509.34 J/h for head and neck, -13873.86 J/h for cervical and -3950.10 J/h for other forms of cancers. Evaporative heat loss was -10949.40 J/h for non-cancer patients, -11326.39 J/h for breast, -11229.40

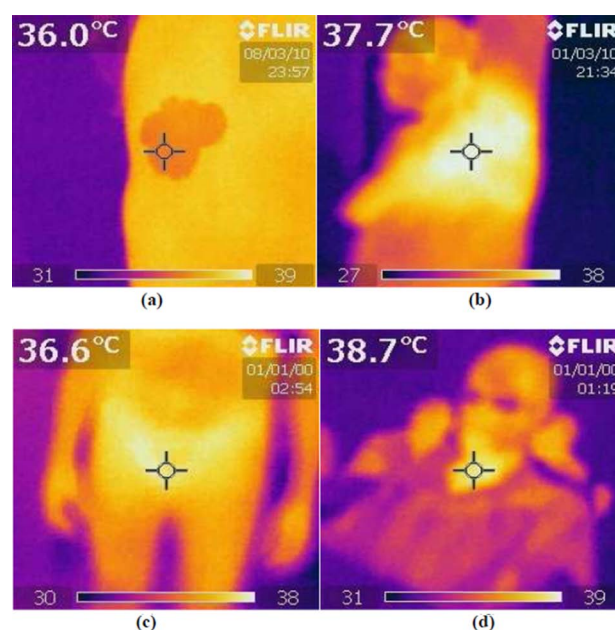


**Figure 7.** Typical thermographs of cancer patients: (a) is Keloid on the left arm, (b) is Cancer of the left breast post-mastectomy, (c) is the Cancer of the cervix and (d) is the Cancer of the thyroid<sup>5</sup>.

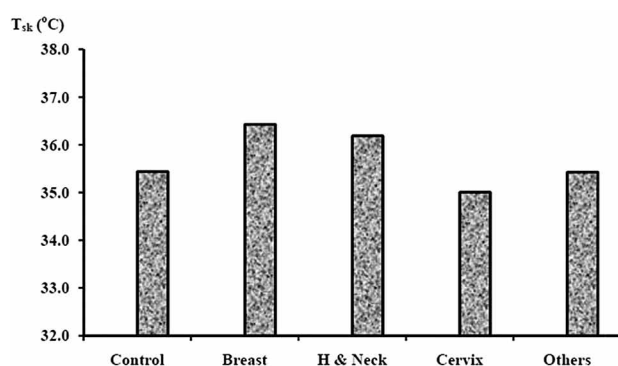


**Figure 8.** Mean value of skin temperature  $T_{sk}$  of cancer patient compared with control<sup>5</sup>.

J/h for head and neck, -10788.62 J/h for cervical and -10946.63 J/h for other forms of cancers. Respirative rate of heat loss was - 6.89 J/h for non-cancer patients, - 6.08 J/h for breast, -5.85 J/h head and neck, -5.35 J/h for cervical patients and -5.87 J/h for other forms of

cancers. Mean skin temperature for non-cancer patients was 35.44°C, for patients with breast cancer 36.43°C, head and neck cancer 36.19°C, cervical 35.01°C and for other forms of cancers it was 35.43°C. Figure 7 shows the aforementioned cancerous parts. The results showed that cancer patients consume less oxygen and gain heat at a higher rate than the non-cancer patients. Skin temperature combined with related physiological energy parameters could be useful in assessing and monitoring cancer patients (Figure 8 and table 4)<sup>5</sup>.

## References

1. Ansari MA, Mohajerani E. Mechanisms of Laser-Tissue Interaction: I. Optical Properties of Tissue, J Lasers Med Sci 2011; 2(3):119-25.
2. Neimz MH. Laser-tissue interactions: Fundamentals and applications. 3rd edn. Berlin: Springer, 2003.
3. Kelly TS. Unjust criticism of the laser. Br J Ophthalmol 1967; 51:641.

**Table 4.** Cancer distribution by site, sex, stage and skin temperature. (Continued on the next page)<sup>5</sup>

Cancer Type	Mean Tsk (°C)	Stage (Freq)	Male Freq (%)	Female Freq (%)	Total Freq (%)
Breast Cancer	36.34	I (5)	1 (0.93)	40 (37.38)	41 (38.32)
	36.48	II (16)			
	37.52	III (6)			
	34.92	IV (5)			
	36.49	NS (9)			
Cervix	33.70	I (1)	-	17 (15.89)	17 (15.89)
	35.93	II (4)			
	35.89	III (7)			
	34.73	IV (4)			
	37.70	NS (1)			
Head & Neck	37.83	II (3)	14 (13.08)	10 (9.35)	24 (22.43)
	37.12	III (5)			
	35.28	IV (5)			
	37.04	NS (11)			
Soft tissue sarcoma	37.50	II (1)	2 (1.87)	2 (1.87)	4 (3.74)
	20.90	IV (2)			
	36.00	NS (1)			
Colorectal	37.10	III (1)	1 (0.93)	1 (0.93)	2 (1.87)
	37.40	IV (1)			
Childhood	32.40	III (1)	1 (0.93)	1 (0.93)	2 (1.87)
	36.30	IV (1)			
Anal	29.00	NS (1)	1 (0.93)	1 (0.93)	2 (1.87)
Rectal	34.60	II (1)	1 (0.93)	2 (1.87)	3 (2.80)
	26.40	NS (1)			
Skin inclusive	35.00	II (1)	4 (3.74)	-	4 (3.74)
	35.60	NS (3)			
Prostate	36.35	II (2)	5 (4.67)	-	5 (4.67)
	34.90	III (1)			
	30.00	IV (1)			
	33.90	NS (1)			
Others	38.00	III (1)	2 (1.87)	3 (2.80)	5 (4.67)
	35.60	IV (1)			
	36.50	NS (3)			
Total			32 (29.88)	75 (72.88)	107 (100)

4. Ring E.F.J., Ammer K. The technique of infrared imaging in medicine. *Thermology international* 2000; 10: 7-14.
5. Ng EYK. A review of thermography as promising non-invasive detection modality for breast tumor. *Int J Therm Sci* 2009; 48 849-59.
6. Aweda MA, Ketiku KK, Ajekigbe AT, Edi AA. Potential role of thermography in cancer management. *Arch Appl Sci Res* 2010; 2 (6):300-12.
7. Ammer K, Melnizky P, Rathkolb O. Skin temperature after intake of sparkling wine, still wine or sparkling water. *Thermol Int* 2003;13 (3):99-102.
8. Ammer K, Ring EFJ. Standard procedures for infrared imaging in medicine, in: *Biomedical Engineering Handbook*, CRC Press, 2006 (Chapters 36-1 to 36-14).
9. Anbar M, Milesescu L, Grenn MW, Zamani K, Marina MT. Study of skin hemodynamics with fast dynamic area telethermometry (DAT). *Proc. 19th Int. Conf. IEEE/EMBS* Oct. 30-Nov. 2, 1997, Chicago, IL, Paper 644, ISBN 0-7803-4265-8 available: CD ROM, ISSN 1094-687X.
10. Archer F, Gros C. Classification thermographique des cancers mammaires, *Bull. Cancer* 1971;58: 351-61.
11. Bhatia V, Bhatia R, Dhindsa S, Dhindsa M. Imaging of the vulnerable plaque: new modalities. *South Med J* 2003; 96 (11): 1142-7.
12. Breast Cancer Foundation (BCF), <http://www.bcf.org.sg/> (last accessed Jan. 2007).
13. Brooks JP, Perry WB, Putnam AT, Karulf RE. Thermal imaging in the detection of bowel ischemia. *Dis Colon Rectum* 2000; 43 (9): 1319-21.
14. Burnay SG, Williams TL, Jones CH. *Applications of Thermal Imaging*. IOP Publishing Ltd., Philadelphia, 1988.
15. Carter SA, Tate RB. Value of toe pulse waves in addition to systolic pressures in the assessment of the severity of peripheral arterial disease and critical limb ischemia. *J Vasc Surg* 1996; 24 (2): 258-65.
16. Clark AT, Mangat JS, Tay SS, King Y, Monk CJ, White PA, et al. Facial thermography is a sensitive and specific method for assessing food challenge outcome. *Allergy* 2007; 62 (7): 744-9.
17. Collins AJ, Notarianni LJ, Ring EF, Seed MP. Some observations on the pharmacology of 'deep-heat', a topical rubifacient. *Ann Rheum Dis* 1984; 43 (3): 411-5.
18. Corvi A, Innocenti B, Mencucci R. Thermography used for analysis and comparison of different cataract surgery procedures based on phacoemulsification. *Physiol Meas* 2006; 27 (4): 371-84.
19. Daniels JW, Molé PA, Shaffrath JD, Stebbins CL. Effects of caffeine on blood pressure, heart rate, and forearm blood flow during dynamic leg exercise. *J Appl Physiol* 1998; 85 (1) 154-9.
20. Fok SC, Ng EYK, Tai K. Early detection and visualization of breast tumor with thermogram and neural network. *J Mech Med Biol* 2002; 2 (2): 185-96.
21. Fok SC, Ng EYK, Thimm GL. Developing case-based reasoning for discovery of breast cancer. *J Mech Med Biol* 2003; 3 (3-4): 231-46.
22. Gautherie M, Kotewicz A, Gueblez P. Accurate and objective evaluation of breast thermograms: basic principles and new advances with special reference to an improved computer-assisted scoring system. in: *Thermal Assessment of Breast Health*, MTP Press Limited, 1983, pp. 72-97.
23. Gautherie M. Thermobiological assessment of benign and malignant breast diseases. *Am J Obstet Gynecol* 1983; 147 (8): 861-9.
24. Gershon-Cohen J, Haberman JD. Thermography of smoking. *Arch. Environ Health* 1968; 16: 637-41.
25. Gold JE, Cherniack M, Buchholz B. Infrared thermography for examination of skin temperature in the dorsal hand of office workers. *Eur J Appl Physiol* 2004; 93 (1-2): 245-51.
26. Gautherie M, Gros C. Breast thermography and cancer risk prediction. *Cancer* 1980; 45: 51-6.
27. Hatcher DJ, D'Andrea JA. Effects on thermography due to the curvature of the porcine eye *InfraMation*. Symposium at Infrared Training Center (ITC) 092-A 2003-08-15,2003, <http://www.infraredtraining.com/store/infra2003.asp> (last accessed 5 Feb. 2008).
28. Ijzerman RG, Serne EH, van Weissenbruch MM, de Jongh RT, Stehouwer CD. Cigarette smoking is associated with an acute impairment of microvascular function in humans. *Clin Sci (Lond)* 2003; 104 (3): 247-52.
29. Kienzler JL, Magnette J, Queille-Roussel C, Sanchez-Ponton A, Ortonne JP. Diclofenac-Na gel is effective in reducing the pain and inflammation associated with exposure to ultraviolet light—results of two clinical studies. *Skin Pharmacol Physiol*. 2005; 18 (3): 144-52.
30. Koot P, Deurenberg P. Comparison of changes in energy expenditure and body temperatures after caffeine consumption. *Ann Nutr Metab* 1995;39 (3): 135-42.
31. Hobbins WB, Ammer K. Controversy: why is a paretic limb cold: High activity of the sympathetic nerve system or weakness of the muscles? *Thermol Österr* 1996; 6: 42-5.
32. Houdas Y, Ring EFJ. *Human Body Temperature—Its Measurement and Regulation*. Plenum Press, New York, 1982.
33. Jay E, Karpman H. Computerized breast thermography. in: *Thermal Assessment of Breast Health*, MTP Press Ltd., 1983, pp. 98-109.
34. Jiang LJ, Ng EYK, Yeo ACB, Wu S, Pan F, Yau WY, et al. A perspective on medical IR imaging. *Int. J Med Eng Technol* 2005; 29 (6): 257-67.
35. Jones CH. Thermography of the female breast, in: C.A. Parsons (Ed.), *Diagnosis of Breast Disease*. University Park Press, Baltimore, 1983, pp. 214-34.
36. Kwon YB, Kim JH, Yoon JH, Lee JD, Han HJ, Mar WC, et al. The analgesic efficacy of bee venom acupuncture for knee osteoarthritis: A comparative study with needle acupuncture. *Am J Chin Med* 2001; 29 (2): 187-99.



37. Keith LG, Oleszczuk JJ, Laguens M. Circadian rhythm chaos: A new breast cancer marker. *Int J Fertil Womens Med* 2001; 46 (6): 238–47.
38. Kerr J. Review of the effectiveness of infrared thermal imaging (thermography) for population screening and diagnostic testing of breast cancer. New Zealand Health Technology Assessment (NZHTA) Tech. Brief Series 3 (3), 2004, [http://nzhta.chmeds.ac.nz/thermography\\_breastcancer.pdf](http://nzhta.chmeds.ac.nz/thermography_breastcancer.pdf) (Last accessed Aug. 2007).
39. Keyserlingk JR, Ahlgren PD, Yu E, Belliveau N. Infrared imaging of breast: Initial reappraisal using high-resolution digital technology in 100 successive cases of stage I and II breast cancer. *Breast J* 1998; 4 (4): 241–51.
40. Keyserlingk JR, Ahlgren PD, Yu E, Belliveau N, Yassa M. Functional infrared imaging of the breast: Historical perspectives, current application and future considerations. *Bomedical Engineering Handbook*, CRC Press, 2006 (Chapters 26-1 to 26-30).
41. Lawson R. Implications of surface temperatures in the diagnosis of breast cancer. *Can Med Assoc J* 1956; 75: 309–11.
42. Lawson R. Thermography—a new tool in the investigation of breast lesions. *Can Serv Med* 1957; 13: 517–24.
43. Lawson RN, Chughtai MS. Breast cancer and body temperatures. *Can Med Assoc J* 1963; 88: 68–70.
44. Lawson RN. A new infrared imaging device. *Can Med Assoc J* 1958; 79: 402–3.
45. Louis K, Walter J, Gautherie M. Long-term assessment of breast cancer risk by thermal imaging. *Biomedical Thermology*, Alan R. Liss Inc., 1982, pp. 279–301.
46. Mannara G, Salvatori GC, Pizzuti GP. Ethyl alcohol induced skin temperature changes evaluated by thermography: Preliminary results, *Boll Soc Ital Biol Sper* 1993; 69 (10): 587–94.
47. Marty W. Thermographie in der Gerichtsmedizin: Anwendungsbeispiele. *Thermo Med* 1990; 6: 67–70.
48. Melnizky P, Ammer K, Scharfemüller T. Thermographische Überprüfung der Heilgymnastik bei Patienten mit Peroneusparese. *Thermol Österr* 1995; 5: 97–102.
49. Melnizky P, Ammer K. Einfluss von Alkohol und Rauchen auf die Hauttemperatur des Gesichts, der Hände und der Kniegelenke. *Thermol Int* 2000; 10 (4): 191–5.
50. Merla A, Di Donato L, Di Luzio S, Farina G, Pisarri S, Proietti M, et al. Infrared functional imaging applied to Raynaud's phenomenon. *IEEE Eng Med Biol Mag* 2002; 21 (6): 73–9.
51. Ng EYK, Fok SC, Peh YC, Ng FC, Sim LS. Computerized detection of breast cancer with artificial intelligence and thermograms. *J Med Eng Technol* 2002; 26 (4): 152–7.
52. Ng EYK, Fok SC. A framework for early discovery of breast tumor using thermography with artificial neural network. *Breast J* 2003; 9 (4): 341–3.
53. Ng EYK, Kaw GJL, Chang WM. Analysis of IR thermal imager for mass blind fever screening. *Microvasc Res* 2004; 68 (2): 104–9.
54. Ng EYK. Is thermal scanner losing its bite in mass screening of fever due to SARS? *Med Phys* 2005; 32 (1): 93–7.
55. Ng EYK, Chen Y, Ung LN. Computerized breast thermography: Study of image segmentation and temperature cyclic variations. *J Med Eng Technol* 2001; 25 (1): 12–6.
56. Ng EYK, Ung LN, Ng FC, Sim LSJ. Statistical analysis of healthy and malignant breast thermography. *J Med Eng Technol* 2001; 25 (6): 253–63.
57. Ng EYK, Sudharsan NM. An improved 3-D direct numerical modeling and thermal analysis of a female breast with tumour. *Proc Inst Mech Eng H* 2001; 215 (1): 25–37.
58. Ng EYK, Sudharsan NM. Effect of blood flow, tumour and cold stress in a female breast: A novel time-accurate computer simulation. *Proc Inst Mech Eng H* 2001; 215 (H4): 393–404.
59. Ng EYK, Chua LT. Prediction of skin burn injury, Part 1: Numerical modeling. *Proc Inst Mech Eng H* 2002; 216 (H3): 157–70.
60. Ng EYK, Chua LT. Prediction of skin burn injury, Part 2: Parametric and sensitivity analysis. *Proc Inst Mech Eng H* 2002; 216 (H3): 171–84.
61. Ng EYK, Chua LT. Comparison of one- and two-dimensional programmes for predicting the state of skin burns. *Burns* 2002; 28 (1): 27–34.
62. Ng EYK, Sudharsan NM. Numerical modelling in conjunction with thermography as an adjunct tool for breast tumour detection. *BMC Cancer* 2004; 4 (17): 1–26.
63. Ng EYK, Chen Y. Segmentation of breast thermogram: Improved boundary detection with modified snake algorithm. *J Mech Med Biol* 2006; 6 (2): 123–36.
64. Ng EYK, Kee EC. Advanced integrated technique in breast cancer thermography. *J Med Eng Technol* 2008; 32 (2): 103–114.
65. Wiecek B, Strzelecki M, Jakubowska T, Wysocki M, Drews-Peszyński C. Advanced thermal image processing. *Biomedical Engineering Handbook*, CRC Press, 2006 (Chapters 28-1 to 28-13).
66. Xu F, Lu TJ, Seffen KA. Biothermomechanical behavior of skin tissue. *Acta Mech Sinica* 2008; 24 (1), doi: 10.1007/s10409-007-0128-8.